Available online at www.sciencedirect.com

ScienceDirect

Ceramics International 41 (2015) 1641–1645

CERAMICS INTERNATIONAL

www.elsevier.com/locate/ceramint

Electronic structure of conducting Al-doped ZnO films as a function of Al doping concentration

Hyun-Woo Park[a], Kwun-Bum Chung[a,*], Jin-Seong Park[b], Seungmuk Ji[c], Kyungjun Song[c], Hyuneui Lim[c], Moon-Hyung Jang[d]

[a]Division of Physics and Semiconductor Physics, Dongguk University, Seoul 100-715, Republic of Korea
[b]Departments of Materials Science and Engineering, Hanyang University, Seoul 133-791, Republic of Korea
[c]Department of Nature-Inspired Nanoconvergence Systems, Korea Institute of Machinery and Materials, 156 Gajeongbuk-Ro, Daejeon 305-343, Republic of Korea
[d]Department of Materials Science and Engineering, University of Pennsylvania, 3231 Walnut Street, Philadelphia, PA 19104, USA

Received 23 August 2014; received in revised form 16 September 2014; accepted 18 September 2014
Available online 28 September 2014

Abstract

Transparent conducting Al-doped ZnO films were deposited by atomic layer deposition with various of Al doping concentrations. In order to explain the change in resistivity of Al-doped ZnO films depending on Al doping concentration, we investigated the correlations between the conducting property and electronic structure in terms of atomic configuration, the evolution of the conduction band and band gap, and band alignments (conduction band offset between minimum of conduction band and Fermi level, ΔE_{CB}). ZnO film Al-doped at ~3 at% and deposited at 250 °C showed the lowest resistivity, which resulted in changes in the conduction band of insulating Al_2O_3 film, and increases in the band gap and conduction band offset (ΔE_{CB}).

Keywords: Electronic structure; Al-doped ZnO; Al doping concentration; Conducting mechanism

1. Introduction

Transparent conducting oxide (TCO) films have recently attracted significant interest in terms of their technological realization for optical and electrical applications such as photovoltaic devices (PVs), organic light-emitting diodes (OLEDs) and transparent thin-film transistors (TFTs) [1–3]. To utilize TCO thin films, there needs to be low resistivity ($\sim 10^{-3}\,\Omega$ cm), high transmittance ($>80\%$) in the visible region and high thermal/chemical stability [4]. In most cases, indium tin oxide (ITO) film has been widely employed as the TCO film due to its good electrical and optical properties, e.g., a low resistivity of $\sim 2\times 10^{-4}\,\Omega$ cm and high transmittance of $>85\%$ [5]. However ITO film has some drawbacks, such as the high cost of indium and its lower wet etch rate compared with those of ZnO or indium gallium zinc oxide (IGZO), which can lead to damage in the active layer [6]. Therefore alternative TCO films that have similar or better properties are needed, and research has been carried out in this area [6].

To overcome the various undesirable properties of ITO, aluminium-doped zinc oxide (AZO) has been intensively studied as a candidate for TCO applications, since it exhibits comparable physical properties to those of ITO, such as a low electrical resistivity of $\sim 10^{-3}\,\Omega$ cm and a high optical transparency of $>80\%$ [6]. Additionally, to obtain high quality AZO with a uniform dopant distribution and good electrical properties, the film fabrication method is very important; atomic layer deposition (ALD) is good technique due to its versatility across various applications. The ALD growth technique can provide good quality film with well-controlled thickness and composition due to its intrinsically self-limiting growth mechanism [7,12]. Given these advantages, Al-doped ZnO films deposited by ALD have been studied in terms of their growth conditions, doping mechanism and their electrical and optical properties [8,9]. However, previous research has focused on

*Corresponding author. Tel.: +82 2 2260 3187.
E-mail address: kbchung@dongguk.edu (K.-B. Chung).

http://dx.doi.org/10.1016/j.ceramint.2014.09.102
0272-8842/

simple changes of electrical properties depending on the Al contents and has explained the electrical conducting properties of AZO films by their physical structure and optical properties [3,9,10]. Yet in addition to the physical and optical changes of AZO films, the origins of conducting properties are strongly correlated to the electronic structure of the film, i.e., the band gap, conduction band, and band alignments. In the present work the electronic structure of AZO films as a function of Al doping concentration is systematically examined, and the associated electrical properties are interpreted.

2. Experiment

An ALD system was employed for the deposition of various Al-doped ZnO films on SiO_2 substrates at substrate temperatures of 250 °C. Diethylzinc (DEZ), Trimethylaluminum (TMA) and de-ionized (DI) water were used as the precursors of Zn, Al, and O respectively. N_2 was used as both the purging and carrier gas, the inlets for which were separated at the side of the chamber. A typical ALD growth sequence for the ZnO layers is composed of exposure to DEZ for 0.2 s, N_2 purging for 20 s and exposure to H_2O for 0.2 s. For the Al_2O_3 layers, exposure to TMA and H_2O for 0.1 s each and purging of the same duration were used. The compositions of Al-doped ZnO films were controlled by changes in the ratio of the supercycle, consisting of the number of cycles of ZnO and Al_2O_3 shown in Fig. 1. Al-doped ZnO films with various Al concentrations were deposited with the thickness of ~45 nm and their compositions were examined by Rutherford backscattering (RBS) and x-ray photoelectron spectroscopy (XPS). To obtain the Zn local atomic bonding nature of Al-doped ZnO films, such as bond lengths and coordination numbers of Zn atoms, Zn K edge extended x-ray fine absorption structure (EXAFS) measurements were performed in beamline 10B1 of the Pohang accelerator laboratory (PAL). In order to understand the conducting properties of Al-doped ZnO as a function of Al doping concentration, the electronic structure of the conduction band and the band alignments (conduction band offset between minimum of conduction band and Fermi level, ΔE_{CB}) was examined by x-ray absorption spectroscopy (XAS), spectroscopic ellipsometry (SE), and x-ray photoelectron spectroscopy (XPS). XAS spectra were measured on the Pohang accelerator laboratory (PAL) beamline 7B1-KIST. SE measurements were performed by a rotating analyzer system with an autoretarder, in the energy range of 0.75–6.4 eV, with incident angles of 65°, 70° and 75°.

3. Results and discussion

To achieve various Al doping concentrations into ZnO films a single TMA-DI water cycle was inserted after a set number of DEZ-DI water cycles at the substrate temperature of 250 °C, which constituted one supercycle of Al-doped ZnO film (AZO) as shown in Fig. 1(a). The supercycles were calculated to target a resultant thickness of ~45 nm for each AZO film. The number of ALD cycles was controlled for the deposition of AZO films with 1, 3, 4, 8 and 10 at% Al, which will hereafter be indexed by AZO 1%, AZO 3%, AZO 4%, AZO 8%, and AZO 10%, respectively. Table 1 shows the Al atomic concentration and film composition of AZO films, as obtained by RBS data of AZO grown on carbon substrate [3].

The electrical properties of the AZO films were investigated by the Hall measurement at room temperature. Fig. 2 shows the resistivity of AZO film as a function of Al doping concentration. The resistivity decreased with the addition of Al until ~3 at% Al and had the lowest value of $4.2 \times 10^{-3}\ \Omega$ cm at ~3 at% Al. Further doping of Al (> ~3 at% Al) results in an increase of resistivity to $1.4 \times 10^{-1}\ \Omega$ cm at AZO 10% film, which represents the parabolic behavior as a function of Al doping concentration. Previous studies regarding the growth of AZO films have reported similar tendencies depending on the Al doping concentration [11,12]. However, their explanations have been focused on changes in physical structure and optical

Table 1
Doped Al doping concentration and composition of Al-doped ZnO films, measured by RBS.

Sample	Al (at%)	Composition
ZnO	0	$Zn_{0.47}\ O_{0.53}$
AZO 3%	3.17	$Al_{0.03}\ Zn_{0.45}\ O_{0.52}$
AZO 4%	3.85	$Al_{0.04}\ Zn_{0.43}\ O_{0.53}$
AZO 10%	10.47	$Al_{0.10}\ Zn_{0.34}\ O_{0.56}$

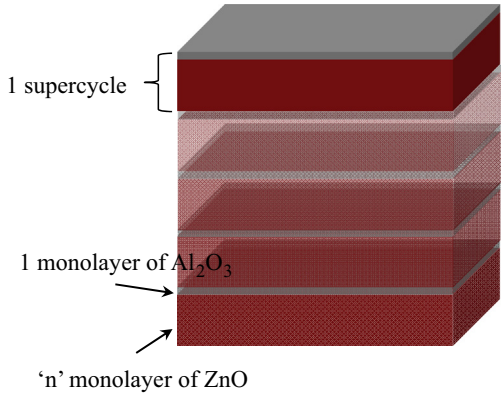

Fig. 1. Schematic diagram of Al-doped ZnO film stack to fabricated with various Al doping concentration by ALD.

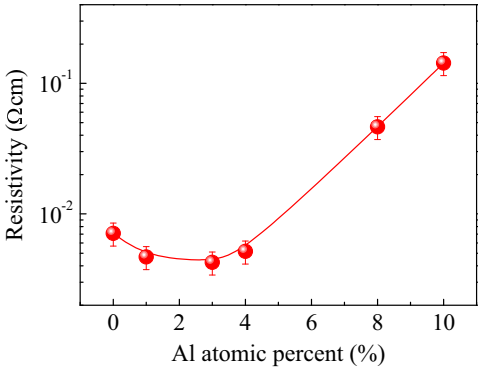

Fig. 2. Resistivity of Al-doped ZnO films as a function of Al doping concentration.

properties. More discussion is provided below in terms of changes in electronic structure and the electrical properties of AZO films as a function of Al concentration. To further verify the local atomic structure around Zn, through EXAFS analysis, the bond lengths and the coordination numbers of Zn, are obtained as shown in Fig. 3 and Table 2. Fitting processes were carried out by FEFF8 and IFFEFIT codes. Zn–Zn bonds are located at peak position of around 3.18 Å while the broad peaks, which are located around 2.02 Å, are due to the Zn–O bond [13,14]. Table 2 shows the bond lengths of Zn–O and Zn–Zn with various Al concentrations as derived from EXAFS data. The undoped ZnO film showed Zn–Zn and Zn–O bonding lengths of 3.1872 Å and 2.0217 Å respectively, a result that is in good agreement with the bond length previously found for bulk ZnO [15]. As the Al concentration increased, the bond length varied within 0.03 Å regardless of Al doping concentration, except in the case of Zn–Zn bond length in AZO 10% film. This indicates that Zn bonds are stable and can maintain their bond character. In the Zn–O bonds, the coordination numbers were increased significantly from 3.2633 to 5.3841 (AZO 3%) while those of the Zn–Zn bonds were decreased from 21.3648 to 14.5625. This result may be due to the Zn–Al bond formation that occurred during the film deposition. As there was Zn–Al bond existence after doping the rest of the Zn atoms form the Zn–O bonds, rather than forming Zn–Zn homopolar bonds. Meanwhile, the coordination numbers for Zn–Zn and Zn–O in AZO 10% film were dramatically decreased to 3.451 and 3.326, respectively. This reduction in the Zn–Zn coordination number indicates that there is continued Zn–Al bond formation. However, the reduction for the coordination number of the Zn–O bond indicates that the rest of the Al atoms form the Al–O bonds in AZO 10% film. This suggests the possibility of certain regions of amorphous insulating material (such as Al_2O_3) at high Al doping concentration, which could lead to a reduction in film conductivity.

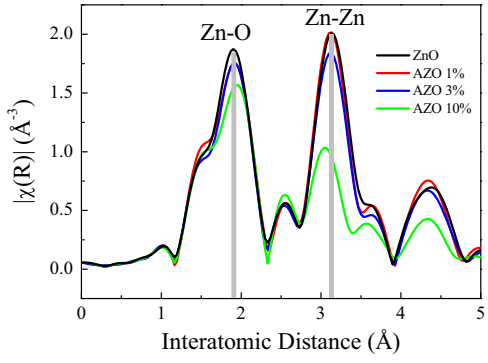

Fig. 3. Fourier transformed EXAFS data of Al-doped ZnO as a function of Al doping concentration, obtained by Zn K edge specta.

Table 2
Bond length and atomic configuration of Zn–O and Zn–Zn, measured by EXFAS.

Sample	Bond	Bond length (Å)	Coordination number	Bond	Bond length (Å)	Coordination number
ZnO	Zn–O	2.02	3.26	Zn–Zn	3.19	21.37
AZO 1%	Zn–O	2.02	4.22	Zn–Zn	3.19	17.60
AZO 3%	Zn–O	2.02	5.38	Zn–Zn	3.18	14.56
AZO 10%	Zn–O	2.05	3.33	Zn–Zn	3.07	3.45

Fig. 4 shows the normalized O K edge spectra of the AZO films as a function of Al doping concentration, as investigated by XAS measurement. The spectra were normalized using the incident beam intensity, I_0, and an x-ray beam background was subtracted from raw data; the differences between the pre- and the post-edge levels were scaled to an arbitrary, but uniform, value [16]. Through normalization of XAS spectra, the qualitative changes and comparison of conduction band features could be analyzed. The normalized O K edge spectra of ZnO and Al_2O_3 are directly related to the oxygen p-projected states of the conduction band, which consists of unoccupied hybridization orbitals for Zn 4sp+O 2p and Al 3sp+O 2p. The O K edge spectra of the AZO 1% and 3% films displayed similar characteristic to that of undoped ZnO film, which means that the dominant electronic structure of the conduction band is that of ZnO film. However, the O K edge spectra of AZO films above 3 at% Al showed noticeable changes and indicated a mixture in electronic structure with ZnO and Al_2O_3 [17]. Compared to the resistivity, the electronic structure of the conduction band can correspond to changes in the conduction property by the incorporation of insulating Al_2O_3. In addition the features of the conduction band reflect the electron conduction transport in unoccupied states, which were modified and shrunk in the low energy region of the conduction band with an increase in the Al doping concentration.

Fig. 5(a) shows the absorption coefficient spectra of AZO films as a function of Al doping concentration. As the doped Al concentration increased, the band gap (E_g) of AZO films

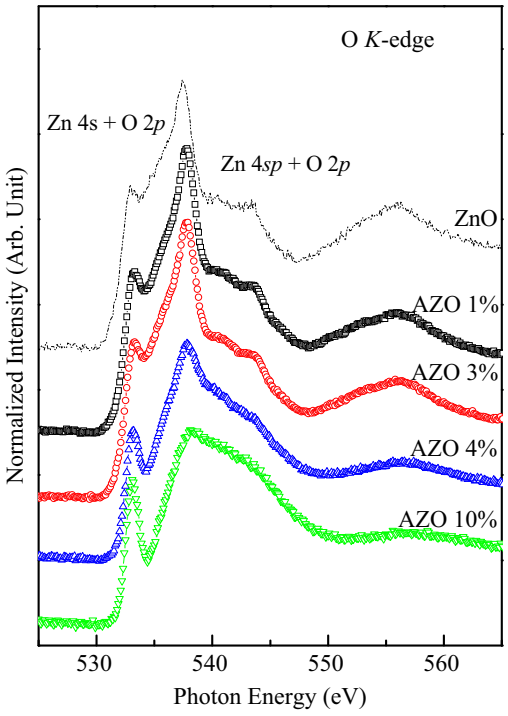

Fig. 4. O K edge spectra of Al-doped ZnO films as a function of Al doping concentration.

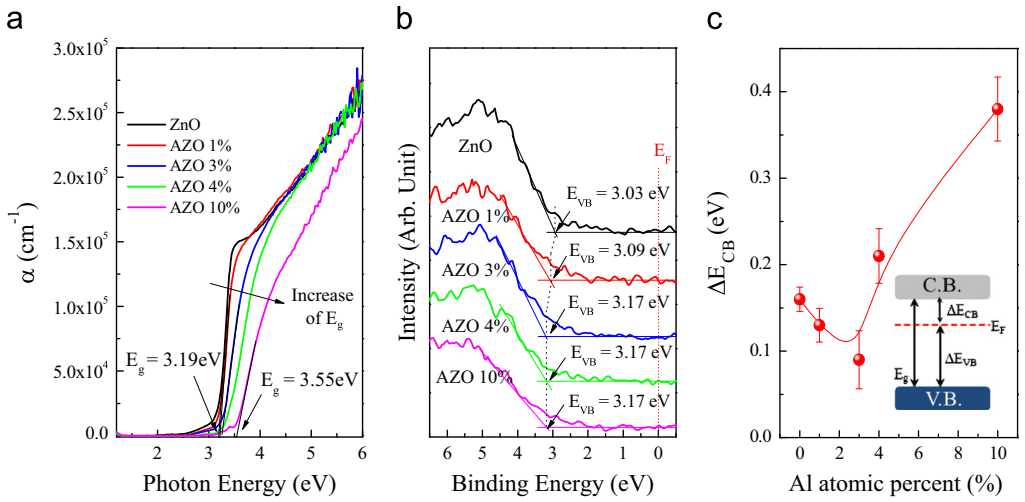

Fig. 5. (a) Absorption coefficient spectra, (b) valence spectra, and (c) conduction band offset (ΔE_{CB}) between minimum of conduction band and Fermi level of Al-doped ZnO films as a function of Al doping concentration.

Table 3
Summarized energy level of band gap (E_g) and conduction band offset (ΔE_{CB}) related to the difference between minimum of conduction band and Fermi level.

	ZnO	AZO 1%	AZO 3%	AZO 4%	AZO 10%
E_g (eV)	3.19	3.22	3.26	3.38	3.55
$\Delta E_{VB}=E_g-E_{CB}$ (eV)	3.03	3.09	3.17	3.17	3.17
$\Delta E_{CB}=E_g-E_{VB}$ (eV)	0.16	0.13	0.09	0.21	0.38

increased from 3.19 eV to 3.55 eV for AZO 10%. This increase in the band gap originates from the incorporated Al_2O_3 and it can induce a reduction in the conduction property due to the insulation property of Al_2O_3. Fig. 5(b) shows the valence spectra obtained by XPS measurement, where the binding energy of 0 eV indicates Fermi energy level. Fig. 5(c) and Table 3 provide the conduction band offset (ΔE_{CB}), calculated by $\Delta E_{CB}=E_g-\Delta E_{VB}$. The conduction band offset has the lowest value for AZO 3% film and shows similar parabolic behavior to that of resistivity in Fig. 2. This is the most plausible origin of resistivity in terms of modification to the conduction band, because the energy difference of conduction band offset can be directly correlated to the probability of electron transfer from occupied states to unoccupied states in the conduction band [18,19].

4. Conclusions

The conduction property of atomic layer deposited Al-doped ZnO films was investigated as a function of Al doping concentration. As the Al doping concentration was changed, Al-doped ZnO film with ~3 at%, deposited at 250 °C showed the lowest resistivity ($4.2\times10^{-3}\ \Omega$ cm). Doped Al is well distributed into ZnO films without the change of a bond length of Zn–O and Zn–Zn. EXAFS analysis shows that, the Al atoms form Al–Zn bonds and Al–O bonds in the case of ZnO: Al 10%. Therefore, this indicates that there needs to be an insulating layer of Al–O bonds in this film. Changes to the conduction property can be explained by the differing electronic structure of Al-doped ZnO with Al doping concentration. The conduction band is significantly changed with insulating Al_2O_3 film above ~5 at% Al and the band gap is gradually increased with the increase of Al doping concentration. In addition, Al-doped ZnO film with the lowest resistivity represents the smallest conduction band offset (ΔE_{CB}) and the evolution of conduction band offset shows the similar tendencies to that of resistivity.

Acknowledgment

This research was partially supported by the Basic Science Research Program through the National Research Foundation of Korea (NRF) funded by the Ministry of Education, Science and Technology (NRF-2013R1A1A2A10005186). In addition, financial support was received from the Korea Research Council for Industrial Science and Technology as part of the project "Mass-Production Technology Support Center for Green Energy Devices".

References

[1] O.K. Varghese, M. Paulose, C.A. Grimes, Nat. Nanotechnol 4 (2009) 592.
[2] K.Y. Cheong, N. Muti, S.R. Ramanan, Thin Solid Films 410 (2002) 142.
[3] W.J. Maeng, J.W. Lee, J.H. Lee, K.B. Chung, J.S. Park, J. Phys. D: Appl. Phys 44 (2011) 445305.
[4] M. Oztas, M. Bedir, Thin Solid Films 516 (2008) 1703.
[5] S. Ishibashi, Y. Higuchi, Y. Ota, K. Nakamura, J. Vac. Sci. Technol. A 8 (1990) 1403.
[6] Y.C. Lin, Y.C. Jian, J.H. Jiang, Appl. Surf. Sci. 254 (2008) 2671.
[7] M. Ritala, K. Kukli, A. Rahtu, P. Raisanen, M. Leskela, T. Sajavaara, J. Keinonen, Science 288 (2000) 319.
[8] M.C. Jun, S.U. Park, J.H. Koh, Nano. Res. Lett 7 (2012) 639.
[9] T. Tynell, H. Yamauchi, M. Karppinen, R. Okazaki, I. Terasaki, J. Vac. Sci. Technol. A 31 (2013) 01A109.

[10] M.L. Grilli, A.N. Sytchkova, S. Boycheva, A. Piegari, Phys. Status Solidi A 210 (4) (2013) 748.
[11] J.-S. Na, G. Scarel, G.N. Parsons, J. Phys. Chem. C 114 (2010) 383.
[12] D.J. Lee, H.M. Kim, J.Y. Kwon, H.J. Choi, S.H. Kim, K.B. Kim, Adv. Funct. Mater. 21 (2011) 448.
[13] J.J. Lu, S.Y. Tsai, Y.M. Lu, T.C. Lin, K.J. Gan, Solid. State Commun 149 (2009) 2177.
[14] W. Mu, L.L. Kerr, N.D. Leyarovska, Chem. Phys. Lett. 469 (2009) 318.
[15] Z. Wu, Y. Zhou, X. Zhang, Appl. Phys. Lett. 84 (2004) 4442.
[16] K.B. Chung, J.P. Long, H. Seo, G. Lucovsky, D. Nordlund, J. Appl. Phys. 106 (2009) 074102.
[17] T. Akatsu, C. Scheu, T. Wagner, T. Gemming, N. Hosoda, T. Suga, M. Rühle, Appl. Surf. Sci. 165 (2000) 159.
[18] H.W. Park, B.K. Kim, J.S. Park, K.B. Chung, Appl. Phys. Lett. 102 (2013) 102102.
[19] J.S. Park, K.C. Ok, B.D. Ahn, J.H. Lee, J.W. Park, K.B. Chung, J. S. Park, Appl. Phys. Lett. 99 (2011) 142104.